

Generalized State-Dependent Exploration for Deep Reinforcement Learning in Robotics

Antonin Raffin

Robotics and Mechatronics Center (RMC)
German Aerospace Center (DLR) Germany
antonin.raffin@dlr.de

Freek Stulp

Robotics and Mechatronics Center (RMC)
German Aerospace Center (DLR) Germany
freek.stulp@dlr.de

Abstract:

Reinforcement learning (RL) enables robots to learn skills from interactions with the real world. In practice, the unstructured step-based exploration used in Deep RL – often very successful in simulation – leads to jerky motion patterns on real robots. Consequences of the resulting shaky behavior are poor exploration, or even damage to the robot. We address these issues by adapting state-dependent exploration (SDE) [1] to current Deep RL algorithms. To enable this adaptation, we propose three extensions to the original SDE, which leads to a new exploration method *generalized state-dependent exploration* (gSDE). We evaluate gSDE both in simulation, on PyBullet continuous control tasks, and directly on a tendon-driven elastic robot. gSDE yields competitive results in simulation but outperforms the unstructured exploration on the real robot. The code is available at <https://github.com/DLR-RM/stable-baselines3/tree/sde>.

Keywords: Robotics, Reinforcement Learning, Exploration

1 Introduction

One of the first robots that used artificial intelligence methods was called “Shakey”, because it would shake a lot during operation [2]. Shaking has now again become quite prevalent in robotics, but for a very different reason. When learning robotic skills with deep reinforcement learning (Deep RL), the de facto standard for exploration is to sample a noise vector ϵ_t from a Gaussian distribution independently at each time step t , and then adding it to the policy output.

$$\epsilon_t \sim \mathcal{N}(0, \sigma^2) \quad \text{Noise sampled from Gaussian at each time step} \quad (1)$$

$$\mathbf{a}_t = \mu(\mathbf{s}_t; \theta_\mu) + \epsilon_t \quad \text{Perturb policy output (action) at each time step} \quad (2)$$

This approach can be very effective in simulation [3, 4, 5, 6, 7], and has therefore also been applied to robotics [8, 9, 10]. But for experiments on real robots, such unstructured exploration has many drawbacks, which have been pointed out by the robotics community [1, 11, 12, 13, 14]:

1. sampling independently at each step leads to shaky behavior [15], and noisy, jittery trajectories
2. the jerky motion patterns can damage the motors on a real robot, and lead to increased wear and tear.
3. in the real world, the system acts as a low pass filter. Thus, consecutive perturbations may cancel each other, leading to poor exploration. This is particularly true for high control frequency [16].
4. it causes a large variance which grows with the number of time-steps [11, 12, 13]

To illustrate those limitations, we will first show a failure case of a state-of-the-art algorithm, Soft Actor-Critic (SAC) [17], on the continuous version of the mountain car problem [18, 19]. Although low-dimensional (2-dimensional state and 1-dimensional action), this environment was shown to be

challenging for DDPG [20]. Despite hyperparameter optimization, the problem cannot be solved without external noise ¹. Because of the unstructured exploration, the commanded power oscillates at high frequency (cf Figure 1), making the velocity stay around the initial value of zero. The policy thus converges to a local minimum of doing nothing, which minimizes the consumed energy.

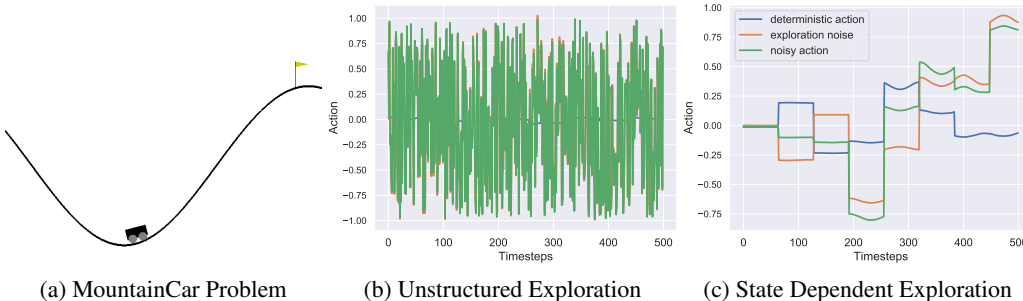


Figure 1: The MountainCar problem. (a) An underpowered car must drive up the mountain to the flag on the right. This requires driving back-and-forth to build up momentum. (b) and (c) illustrate the exploration during the first 500 steps. Unstructured exploration (b) produces high-frequency noise while SDE (c) provides smooth and consistent exploration, allowing the top of the mountain to be reached. The action executed is decomposed into its deterministic and exploratory component.

In robotics, multiple solutions have been proposed to counteract this inefficient exploration strategy. These include correlated noise [8, 16], low-pass filters [21, 22], action repeat [23] or lower level controllers [21, 9]. A more principled solution is to perform exploration in parameter space, rather than in action space [24, 25]. This approach usually requires fundamental changes in the algorithm, and is harder to tune when the number of parameters is high.

State Dependent Exploration (SDE) [1, 12] was proposed as a compromise between exploring in parameter and action space. SDE replaces the sampled noise with a state-dependent exploration function, which during an episode returns the same action for a given state. This results in smoother exploration and less variance per episode. To the best of our knowledge, no Deep RL algorithm has yet been successfully combined with SDE. We surmise that this is because the problem that it solves – shaky, jerky movement – is not as noticeable in simulation, which is the current focus of the community.

Going back to the MountainCar problem, SAC with SDE can solve it with many different hyperparameter configurations ². Looking at the taken actions during early stage of training (cf Figure 1), it is clear that State Dependent Exploration provides a smoother and more consistent exploration, permitting to drive up the hill.

In this paper, we aim at reviving interest in SDE as an effective method for addressing exploration issues that arise from using independently sampled Gaussian noise on real robots. Our concrete contributions, which also determine the structure of the paper, are:

1. highlighting the issues with unstructured Gaussian exploration (Section 1).
2. adapting SDE to recent Deep RL algorithms, and addressing some issues of the original formulation (Section 2.2).
3. providing a full benchmark with tuned hyperparameters of recent model-free algorithms on the open source PyBullet [26] continuous control environments (Section 4.1).
4. performing an ablation study for SDE (Section 4.2).
5. successfully applying RL directly on a tendon-driven robot, without the need of a simulator or filters (Section 4.3).

¹See issue on the original SAC repository <https://frama.link/original-sac-mountaincar>

²See report <https://frama.link/MountainCarSDEHyperparametersReport>

2 Background

In reinforcement learning, an agent interacts with its environment, usually modeled as a Markov Decision Process (MDP) $(\mathcal{S}, \mathcal{A}, p, r)$ where \mathcal{S} is the state space, \mathcal{A} the action space and $p(s'|s, \mathbf{a})$ the transition function. At every step t , the agent performs an action \mathbf{a} in state s following its policy $\pi : \mathcal{S} \mapsto \mathcal{A}$. It then receives a feedback signal in the next state s' : the reward $r(s, \mathbf{a})$. The objective of the agent is to maximize the long-term reward. More formally, the goal is to maximize the expectation of the sum of discounted reward, over the trajectories ρ_π generated using its policy π :

$$\sum_t \mathbb{E}_{(\mathbf{s}_t, \mathbf{a}_t) \sim \rho_\pi} [\gamma^t r(\mathbf{s}_t, \mathbf{a}_t)] \quad (3)$$

where $\gamma \in [0, 1]$ is the discount factor and represents a trade-off between maximizing short-term and long-term rewards. The agent-environment interactions are often broken down into sequences called *episodes*, that end when the agent reaches a terminal state.

2.1 Exploration in action or policy parameter space

In the case of continuous actions, the exploration is commonly done in the *action space* [27, 28, 29, 30, 31, 6]. At each time-step, a noise vector ϵ_t is independently sampled from a Gaussian distribution and then added to the controller output.

$$\mathbf{a}_t = \mu(\mathbf{s}_t; \theta_\mu) + \epsilon_t, \quad \epsilon_t \sim \mathcal{N}(0, \sigma^2) \quad (4)$$

where $\mu(\mathbf{s}_t)$ is the deterministic policy and $\pi(\mathbf{a}_t | \mathbf{s}_t) \sim \mathcal{N}(\mu(\mathbf{s}_t), \sigma^2)$ is the resulting stochastic policy, used for exploration. θ_μ denotes the parameters of the deterministic policy. For simplicity, throughout the paper, we will only consider Gaussian distributions with diagonal covariance matrices. Hence, here, σ is a vector with the same dimension as the action space \mathcal{A} .

Alternatively, the exploration can also be done in the *parameter space* [12, 24, 25, 32]. At the beginning of an episode, the perturbation ϵ is sampled and added to the policy parameters θ_μ . This usually results in more consistent exploration but becomes challenging with an increasing number of parameters [24].

$$\mathbf{a}_t = \mu(\mathbf{s}_t; \theta_\mu + \epsilon), \quad \epsilon \sim \mathcal{N}(0, \sigma^2) \quad (5)$$

2.2 State Dependent Exploration

State Dependent Exploration (SDE) [1, 12] is an intermediate solution that consists in adding noise as a function of the state \mathbf{s}_t , to the deterministic action $\mu(\mathbf{s}_t)$. At the beginning of an episode, the parameters θ_ϵ of that exploration function are drawn from a Gaussian distribution. The resulting action \mathbf{a}_t is as follows:

$$\mathbf{a}_t = \mu(\mathbf{s}_t; \theta_\mu) + \epsilon(\mathbf{s}_t; \theta_\epsilon), \quad \theta_\epsilon \sim \mathcal{N}(0, \sigma^2) \quad (6)$$

In the linear case, i. e. with a linear policy and a noise matrix, parameter space exploration and SDE are equivalent:

$$\begin{aligned} \mathbf{a}_t &= \mu(\mathbf{s}_t; \theta_\mu) + \epsilon(\mathbf{s}_t; \theta_\epsilon), & \theta_\epsilon &\sim \mathcal{N}(0, \sigma^2) \\ &= \theta_\mu \mathbf{s}_t + \theta_\epsilon \mathbf{s}_t \\ &= (\theta_\mu + \theta_\epsilon) \mathbf{s}_t \end{aligned}$$

This episode-based exploration is smoother and more consistent than the unstructured step-based exploration. Thus, during one episode, instead of oscillating around a mean value, the action \mathbf{a} for a given state \mathbf{s} will be the same.

In the remainder of this paper, to avoid overloading notation, we drop the time subscript t , i. e. we now write \mathbf{s} instead of \mathbf{s}_t . \mathbf{s}_j or \mathbf{a}_j now refer to an element of the state or action vector.

In the case of a linear exploration function $\epsilon(\mathbf{s}; \theta_\epsilon) = \theta_\epsilon \mathbf{s}$, by operation on Gaussian distributions, Rückstieß et al. [1] show that the action element \mathbf{a}_j is normally distributed:

$$\pi_j(\mathbf{a}_j|\mathbf{s}) \sim \mathcal{N}(\mu_j(\mathbf{s}), \hat{\sigma}_j^2) \quad (7)$$

where $\hat{\sigma}$ is a diagonal matrix with elements $\hat{\sigma}_j = \sqrt{\sum_i (\sigma_{ij} \mathbf{s}_i)^2}$

We can then obtain the derivative of the log-likelihood $\log \pi(\mathbf{a}|\mathbf{s})$ with respect to the variance σ :

$$\frac{\partial \log \pi(\mathbf{a}|\mathbf{s})}{\partial \sigma_{ij}} = \sum_k \frac{\partial \log \pi_k(\mathbf{a}_k|\mathbf{s})}{\partial \hat{\sigma}_j} \frac{\partial \hat{\sigma}_j}{\partial \sigma_{ij}} \quad (8)$$

$$= \frac{\partial \log \pi_j(\mathbf{a}_j|\mathbf{s})}{\partial \hat{\sigma}_j} \frac{\partial \hat{\sigma}_j}{\partial \sigma_{ij}} \quad (9)$$

$$= \frac{(\mathbf{a}_j - \mu_j)^2 - \hat{\sigma}_j^2 \mathbf{s}_i^2 \sigma_{ij}}{\hat{\sigma}_j^3 \hat{\sigma}_j} \quad (10)$$

This can be easily plugged into the likelihood ratio gradient estimator [33], which allows to adapt σ during training. SDE is therefore compatible with standard policy gradient methods, while addressing most shortcomings of the unstructured exploration.

For a non-linear exploration function, the resulting distribution $\pi(\mathbf{a}|\mathbf{s})$ is most of the time unknown. Thus, computing the exact derivative w.r.t. the variance is not trivial and may require approximate inference. As we focus on simplicity, we leave this extension for future work.

3 Generalized State Dependent Exploration (gSDE)

Considering Equations (7) and (8), some limitations of the original formulation are apparent:

- i the variance of the policy $\hat{\sigma}_j = \sqrt{\sum_i (\sigma_{ij} \mathbf{s}_i)^2}$ depends on the state space dimension (it grows with it), which means that the initial σ must be tuned for each problem.
- ii there is only a linear dependency between the state and the exploration noise, which limits the possibilities.
- iii the state must be normalized, as the gradient and the noise magnitude depend on the state magnitude, otherwise one may have gradient issues.
- iv the noise does not change during one episode, which is problematic [34] if the episode length is long, because the exploration will be limited.

To mitigate the mentioned issues and adapt it to Deep RL algorithms, we propose three improvements:

1. instead of the state \mathbf{s} , we can in fact use any features. We chose policy features $\mathbf{z}_\mu(\mathbf{s}; \theta_{\mathbf{z}_\mu})$ (last layer before the deterministic output $\mu(\mathbf{s}) = \theta_\mu \mathbf{z}_\mu(\mathbf{s}; \theta_{\mathbf{z}_\mu})$) as input to the noise function $\epsilon(\mathbf{s}; \theta_\epsilon) = \theta_\epsilon \mathbf{z}_\mu(\mathbf{s})$.
2. we sample the parameters θ_ϵ of the exploration function every n steps instead of every episode.
3. when applicable (here, for A2C [29] and PPO [30]), we make use of parallelization and have multiple exploration matrices. That is to say, for each worker [29], we draw different parameters of the exploration function.

Using *policy features* allows to mitigate issues **i**, **ii** and **iii**: the variance of the policy only depends on the network architecture and the relationship between the state s and the noise ϵ is non-linear. This permits for instance to use images as input. Also, because we can back-propagate through $\mathbf{z}_\mu(s)$ (using the reparametrization trick [35]), the features can be learned.

This formulation is therefore more general and includes the original SDE description. In practice, as encountered during our early experiments, relying on policy features makes the algorithm easier to tune and avoid the use of normalization: the weights of the policy are usually small at the beginning of training and evolve slowly, which mitigates gradient problem.

Sampling the parameters θ_ϵ every n steps tackles the issue **iv**. and yields a unifying framework [34] which encompasses both unstructured exploration ($n = 1$) and original SDE ($n = \text{episode_length}$). This formulation follows the description of Deep RL algorithms that update their parameters every m step. In the remainder of the paper, n is always the same (except for PPO) as the update frequency ($n = m$). This avoids having an additional hyperparameter.

Finally, using multiple exploration matrices for A2C and PPO favor exploration and generally yield better results (cf Section 4.2).

We call the resulting approach *generalized State Dependent Exploration* (gSDE).

Deep RL algorithms Integrating this updated version of SDE into recent Deep RL algorithms, such as those listed in Appendix A.1, is straightforward. For A2C, PPO and SAC, that rely on a probability distribution, we can replace the original Gaussian distribution by the one derived in Equation (7), where the analytical form of the log-likelihood is known (cf Equation (8)). Regarding TD3 [6], which doesn't need any distribution, there is even more freedom in the choice of the exploration function. We chose an on-policy exploration based on A2C gradient update, as it allows to adapt the noise magnitude automatically, instead of relying on a scheduler for instance. We provide pseudo-code for SAC with gSDE in the Appendix A.2

4 Experiments

The goal of this section is to investigate the performance of gSDE compared to unstructured exploration in simulation and on a real system. We first evaluate the two strategies on a set of simulated continuous control tasks. Then, we perform an ablation study to assess the usefulness and robustness of the proposed modifications. Finally, we apply gSDE directly on a real tendon-driven robot and compared it to a model-based controller

4.1 Continuous Control Simulated Environments

Experiment setup In order to compare gSDE to unstructured exploration in simulation, we chose 4 locomotion tasks from the PyBullet [26] environments: HALFCHEETAH, ANT, HOPPER and WALKER2D. They are similar to the one found in OpenAI Gym [19] but the simulator is open source and they are harder to solve³.

We fix the budget to 1 Million steps for off-policy algorithms (SAC, TD3), and to 2 Million for on-policy methods (A2C, PPO) because they require less time to train but are sample inefficient. We report the average score over 10 runs and the associated variance. This variance corresponds to the 68% confidence interval for the estimation of the mean. For each run, we test the learned policy on 10 evaluation episodes every 10000 steps, using the deterministic controller $\mu(s_t)$. In all learning curve figures, unless specified otherwise, the x -axis represents the number of steps performed in the environment.

Regarding the implementation⁴, we use a PyTorch [36] version of Stable-Baselines [37], with performances matching the ones published in the RL zoo [38].

The methodology we follow to tune the hyperparameters can be found in Appendix A.5. PPO and TD3 hyperparameters for unstructured exploration are reused from the original papers [30, 6]. For SAC, the optimized hyperparameters for gSDE are performing better than the ones from Haarnoja et al. [17], so we keep them for the unstructured exploration to have a fair comparison. No

³<https://frama.link/PyBullet-harder-than-MuJoCo-envs>

⁴The code is available at <https://github.com/DLR-RM/stable-baselines3/tree/sde>

hyperparameters are available for A2C in Mnih et al. [29] so we use the tuned one from Raffin [38]. Full hyperparameters details are listed in Appendix A.6.

Environments	A2C		PPO	
	gSDE	Gaussian	gSDE	Gaussian
HALFCHEETAH	2028 +/- 107	1652 +/- 94	2760 +/- 52	2254 +/- 66
ANT	2560 +/- 45	1967 +/- 104	2587 +/- 133	2160 +/- 63
HOPPER	1448 +/- 163	1559 +/- 129	2508 +/- 16	1622 +/- 220
WALKER2D	694 +/- 73	443 +/- 59	1776 +/- 53	1238 +/- 75

Table 1: Final performance (higher is better) of A2C and PPO on 4 environments with gSDE and unstructured Gaussian exploration (higher is better). We report the mean over 10 runs of 2 million steps. For each benchmark, we highlight the results of the method with the best mean.

Environments	SAC		TD3	
	gSDE	Gaussian	gSDE	Gaussian
HALFCHEETAH	2945 +/- 95	2883 +/- 57	2578 +/- 44	2687 +/- 67
ANT	3106 +/- 61	2859 +/- 329	3267 +/- 34	2865 +/- 278
HOPPER	2515 +/- 50	2477 +/- 117	2353 +/- 78	2470 +/- 111
WALKER2D	2270 +/- 28	2215 +/- 92	1989 +/- 153	2106 +/- 67

Table 2: Final performance of SAC and TD3 on 4 environments with gSDE and unstructured Gaussian exploration. We report the mean over 10 runs of 1 million steps.

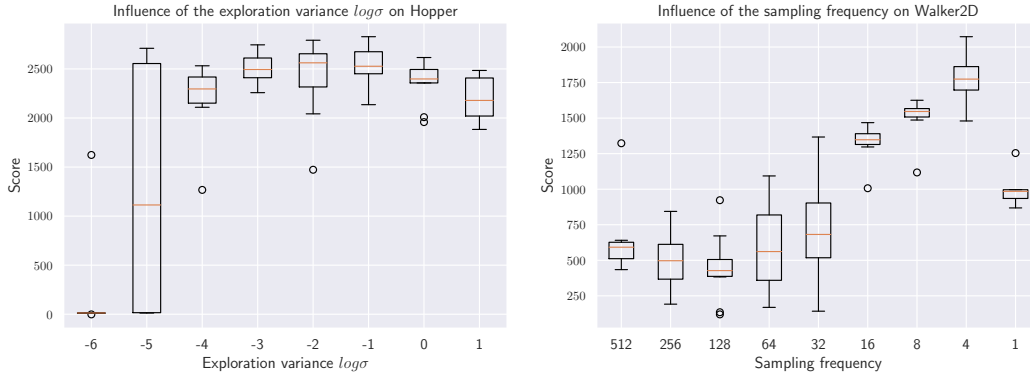
Results The results in Table 1 show that on-policy algorithms with gSDE perform much better than with the unstructured exploration. This difference may be explained by better hyperparameters, as gSDE main advantage is on a real robot. PPO reaches higher scores than A2C which confirms results previously published.

Regarding off-policy algorithms in Table 2, the performance of gSDE is on-par with their independent exploration equivalent. As expected, no real difference is seen in simulation. The essential improvement of gSDE is shown on a real system (cf Section 4.3). The off-policy algorithms are also much more sample efficient compared to their on-policy counterparts: they attain higher performances using half the budget. Those results comfort our choice of SAC for experiments on a real robot.

4.2 Ablation Study

In this section, we investigate the contribution of the proposed modifications to the original SDE: using policy features as input to the noise function, sampling the exploration function parameters every n steps and different exploration parameters per worker. We also examine how sensitive SAC is to the initial exploration variance σ , which is the only additional hyperparameter introduced by SDE. This study is missing in the original paper.

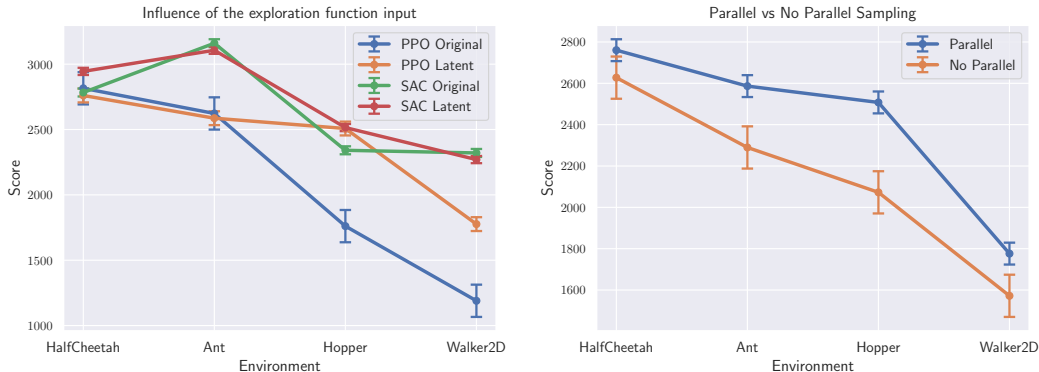
Initial Exploration Variance Robustness to hyperparameter choice is important for experiments in the real world, as hyperparameter tuning would be quite costly. Therefore, we investigate the influence of the initial exploration variance $\log \sigma$ on PyBullet environments. The results for SAC on the HOPPER task is displayed in Figure 2a. SAC is working for a wide range of initial values: from $\log \sigma = -4$ ($\sigma \approx 0.018$) to $\log \sigma = 0$ ($\sigma \approx 1$). This is also the case for the other PyBullet tasks, as shown in Appendix A.4.



(a) Initial exploration variance $\log \sigma$ (SAC on HOPPER) (b) Sampling frequency (PPO on WALKER2D)

Figure 2: Sensitivity of SAC and PPO to selected hyperparameters on PyBullet tasks. (a) SAC works for a wide range of initial exploration variance (b) The frequency of sampling the noise function parameters is crucial for PPO with gSDE.

Sampling frequency gSDE is a n -step version of SDE, where n is set to be the same as the update frequency (except for PPO). This n -step version allows to interpolate between the unstructured exploration $n = 1$ and the original SDE per-episode formulation. Figure 2b shows the importance of that parameter for PPO on the WALKER2D task. If the sampling interval is too large, the agent won't explore enough during long episodes. On the other hand, with a high sampling frequency $n \approx 1$, the issues mentioned in Section 1 arise.



(a) Exploration function input

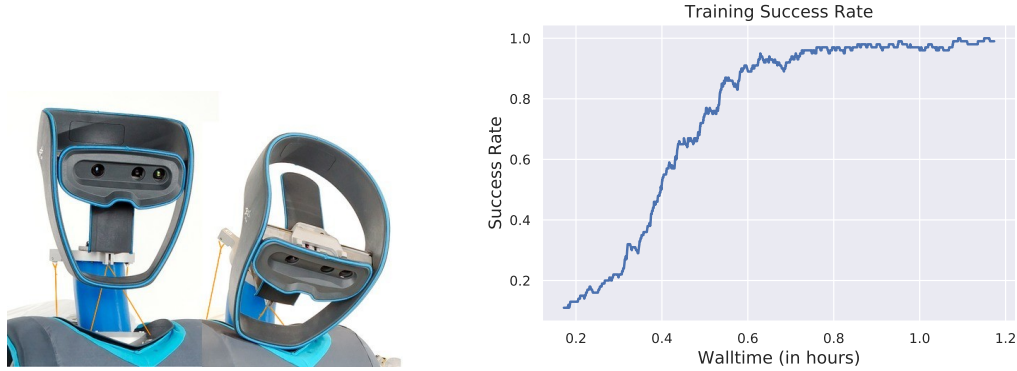
(b) Parallel sampling of the noise parameters

Figure 3: (a) Influence of the input to the exploration function $\epsilon(\mathbf{s}; \theta_\epsilon)$ for SAC and PPO on PyBullet environments: using latent features from the policy \mathbf{z}_μ (Latent) is usually better than using the state \mathbf{s} (Original). (b) Parallel sampling of the noise matrix has a positive impact for PPO on PyBullet tasks.

Policy features as input Figure 3a shows the effect of changing the exploration function input for SAC and PPO. Although it varies from task to task, using policy features is usually beneficial, especially for PPO. It also requires less tuning and no normalization as it depends only on the policy network architecture. Here, the PyBullet tasks are low dimensional and the state space size is of the same order, so no careful per-task tuning is needed. Relying on features also allows to learn directly from pixels, which is not possible in the original formulation.

Parallel Sampling The effect of sampling a set of noise parameters per worker is shown for PPO in Figure 3b. This modification improves the performance for each task, as it allows a more diverse exploration. Although less significant, we observe the same outcome for A2C on PyBullet environments (cf Figure 8). Thus, making use of parallel workers improves both exploration and the final performance.

4.3 Learning to Control a Tendon-Driven Elastic Robot



(a) Tendon-driven elastic continuum neck in a humanoid robot

(b) Training success rate on the real robot

Figure 4: (a) The tendon-driven robot [39] used for the experiment. The tendons are highlighted in orange. (b) Training success rate on the real robot. The blue line is a moving average over 100 episodes and the x-axis is the wall-clock time in hours.

Experiment setup To assess the usefulness of gSDE, we apply it on a real system. The task is to control a tendon-driven elastic continuum neck [39] (see Figure 4a) to a given target pose. Controlling such soft robot is challenging as the deformation of the structure needs to be modeled accurately, which is computationally expensive [40, 41] and requires assumptions.

The system is under-actuated (there are only 4 tendons), hence, the desired pose is a 4D vector: 3 angles for the rotation $\theta_x, \theta_y, \theta_z$ and one for the position x . The input is a 16D vector composed of: the measured tendon lengths (4D), the current tendon forces (4D), the current pose (4D) and the target pose (4D). The reward is a weighted sum between the negative geodesic distance to the desired orientation and the negative Euclidean distance to the desired position. The weights are chosen such that the two components have the same magnitude. The agent receives an additional reward of +2 when reaching and staying at the target pose for half a second. The action space consists in desired delta in tendon forces, limited to 5N. For safety reasons, the tendon forces are clipped below 10N and above 40N. An episode terminates either when the agent reaches the desired pose or after a timeout of 5s, i.e. each episode has a maximum length of 200 steps. The episode is considered successful if the desired pose is reached within a threshold of 2mm for the position and 1deg for the orientation. The agent controls the tendons forces at 30Hz, while a PD controller monitors the motor current at 3KHz on the robot. The gradient update was directly done on a 4-core laptop, after each episode.

Results We first ran the unstructured exploration on the robot but had to stop the experiment early: the high-frequency noise in the command was damaging the tendons and would have broken them due to their friction on the bearings.

Then, we trained a controller using SAC with gSDE for two hours. After one hour, the learned policy could already reach successfully 98% of the desired poses (cf Figure 4b).

5 Related Work

Exploration is a key topic in reinforcement learning [18]. It has been extensively studied in the discrete case and most recent papers still focus on discrete actions [42, 43, 44, 45].

Several works tackle the issues of unstructured exploration for continuous control by replacing it with correlated noise. Korenkevych et al. [16] use an autoregressive process and introduce two variables that allows to control the smoothness of the exploration. In the same vein, van Hoof et al. [34] rely on a temporal coherence parameter to interpolate between the step- or episode-based exploration, making use of a Markov chain to correlate the noise. This smoothed noise comes at a cost: it requires an history, which changes the problem definition.

Exploring in parameter space [11, 46, 12, 13, 47, 48] is an orthogonal approach that also solves some issues of the unstructured exploration. It was successfully applied to real robot but relied on motor primitives [49, 13], which requires expert knowledge. Plappert et al. [24] adapt parameter exploration to Deep RL by defining a distance in the action space and applying layer normalization to handle high-dimensional space. This approach however adds both complexity, as defining a distance in the action space is not trivial, and computational load.

Population based algorithms, such as Evolution strategies (ES) or Genetic Algorithms (GA), also explore in parameter space. Thanks to massive parallelization, they were shown to be competitive [50, 51] with RL in terms of training time, at the cost of being sample inefficient. To address this problem, recent works [32, 25] proposed to combine ES exploration with RL gradient update. This combination, although powerful, unfortunately adds numerous hyperparameters and a non-negligible computational overhead.

6 Conclusion

Motivated by a simple failure case, we highlighted several issues that arise from the unstructured exploration in Deep RL algorithms for continuous control. Due to those issues, these algorithms cannot be directly applied to real-world robotic problems.

To address these issues, we adapt State Dependent Exploration to Deep RL algorithms by extending the original formulation: we replace the exploration function input by learned features, sample the parameters every n steps, and make use of parallelism. This generalized version ($gSDE$), provides a simple and efficient alternative to unstructured Gaussian exploration.

$gSDE$ achieves very competitive results on several continuous control benchmarks. We also investigate the contribution of each modification by performing an ablation study. Our proposed exploration strategy, combined with SAC, is robust to hyperparameter choice, which makes it suitable for robotics applications. To demonstrate it, we successfully apply SAC with $gSDE$ directly on a tendon-driven elastic robot. The trained controller matches the performance of a model-based approach in less than two hours.

Although much progress is being made in *sim2real* approaches, we believe there is still much truth in Rodney Brooks’ assessment that “the world is its own best model”. Reinforcement learning on real robots does not require the modeling of interaction forces, friction due to wear and tear, or sensor errors and failures; all of which are also difficult to cover with domain randomization. For these reasons, we believe more effort should be invested in learning on real systems, even if this poses challenges in terms of safety and duration of learning. This paper is meant as a step towards this goal, and we hope that it will revive interest in developing exploration methods that can be directly applied to real robots.

Acknowledgments

The work described in this paper was partially funded by the project “Reduced Complexity Models” from the “Helmholtz-Gemeinschaft Deutscher Forschungszentren”.

References

- [1] T. Rückstieß, M. Felder, and J. Schmidhuber. State-dependent exploration for policy gradient methods. In *Joint European Conference on Machine Learning and Knowledge Discovery in Databases*, pages 234–249. Springer, 2008.
- [2] N. J. Nilsson. Shakey the robot. Technical Report 323, Artificial Intelligence Center, SRI International, Menlo Park, CA, USA, 1984. URL <http://www.ai.sri.com/shakey/>.
- [3] Y. Duan, X. Chen, R. Houthoof, J. Schulman, and P. Abbeel. Benchmarking deep reinforcement learning for continuous control. In *International Conference on Machine Learning*, pages 1329–1338, 2016.
- [4] X. B. Peng, P. Abbeel, S. Levine, and M. van de Panne. Deepmimic: Example-guided deep reinforcement learning of physics-based character skills. *ACM Transactions on Graphics (TOG)*, 37(4):143, 2018.
- [5] M. Andrychowicz, B. Baker, M. Chociej, R. Jozefowicz, B. McGrew, J. Pachocki, A. Petron, M. Plappert, G. Powell, A. Ray, et al. Learning dexterous in-hand manipulation. *arXiv preprint arXiv:1808.00177*, 2018.
- [6] S. Fujimoto, H. van Hoof, and D. Meger. Addressing function approximation error in actor-critic methods. *arXiv preprint arXiv:1802.09477*, 2018.
- [7] J. Hwangbo, J. Lee, A. Dosovitskiy, D. Bellicoso, V. Tsounis, V. Koltun, and M. Hutter. Learning agile and dynamic motor skills for legged robots. *arXiv preprint arXiv:1901.08652*, 2019.
- [8] T. Haarnoja, A. Zhou, K. Hartikainen, G. Tucker, S. Ha, J. Tan, V. Kumar, H. Zhu, A. Gupta, P. Abbeel, et al. Soft actor-critic algorithms and applications. *arXiv preprint arXiv:1812.05905*, 2018.
- [9] A. Kendall, J. Hawke, D. Janz, P. Mazur, D. Reda, J.-M. Allen, V.-D. Lam, A. Bewley, and A. Shah. Learning to drive in a day. In *2019 International Conference on Robotics and Automation (ICRA)*, pages 8248–8254. IEEE, 2019.
- [10] H. Zhu, J. Yu, A. Gupta, D. Shah, K. Hartikainen, A. Singh, V. Kumar, and S. Levine. The ingredients of real world robotic reinforcement learning. In *International Conference on Learning Representations*, 2020. URL <https://openreview.net/forum?id=rJe2syrtvS>.
- [11] J. Kober and J. R. Peters. Policy search for motor primitives in robotics. In *Advances in neural information processing systems*, pages 849–856, 2009.
- [12] T. Rückstieß, F. Sehnke, T. Schaul, D. Wierstra, Y. Sun, and J. Schmidhuber. Exploring parameter space in reinforcement learning. *Paladyn, Journal of Behavioral Robotics*, 1(1): 14–24, 2010.
- [13] F. Stulp and O. Sigaud. Robot skill learning: From reinforcement learning to evolution strategies. *Paladyn, Journal of Behavioral Robotics*, 4(1):49–61, 2013.
- [14] M. P. Deisenroth, G. Neumann, J. Peters, et al. A survey on policy search for robotics. *Foundations and Trends® in Robotics*, 2(1–2):1–142, 2013.
- [15] A. Raffin and R. Sokolov. Learning to drive smoothly in minutes. <https://github.com/araffin/learning-to-drive-in-5-minutes/>, 2019.
- [16] D. Korenkevych, A. R. Mahmood, G. Vasan, and J. Bergstra. Autoregressive policies for continuous control deep reinforcement learning. *arXiv preprint arXiv:1903.11524*, 2019.
- [17] T. Haarnoja, A. Zhou, P. Abbeel, and S. Levine. Soft actor-critic: Off-policy maximum entropy deep reinforcement learning with a stochastic actor. *arXiv preprint arXiv:1801.01290*, 2018.
- [18] R. S. Sutton and A. G. Barto. *Reinforcement learning: An introduction*. MIT press, 2018.
- [19] G. Brockman, V. Cheung, L. Pettersson, J. Schneider, J. Schulman, J. Tang, and W. Zaremba. Openai gym. *arXiv preprint arXiv:1606.01540*, 2016.

- [20] C. Colas, O. Sigaud, and P.-Y. Oudeyer. Gep-pg: Decoupling exploration and exploitation in deep reinforcement learning algorithms. *arXiv preprint arXiv:1802.05054*, 2018.
- [21] T. Haarnoja, S. Ha, A. Zhou, J. Tan, G. Tucker, and S. Levine. Learning to walk via deep reinforcement learning. *arXiv preprint arXiv:1812.11103*, 2018.
- [22] S. Ha, P. Xu, Z. Tan, S. Levine, and J. Tan. Learning to walk in the real world with minimal human effort. *arXiv preprint arXiv:2002.08550*, 02 2020.
- [23] M. Neunert, A. Abdolmaleki, M. Wulfmeier, T. Lampe, J. T. Springenberg, R. Hafner, F. Romano, J. Buchli, N. Heess, and M. Riedmiller. Continuous-discrete reinforcement learning for hybrid control in robotics. *arXiv preprint arXiv:2001.00449*, 2020.
- [24] M. Plappert, R. Houthoofd, P. Dhariwal, S. Sidor, R. Y. Chen, X. Chen, T. Asfour, P. Abbeel, and M. Andrychowicz. Parameter space noise for exploration. *arXiv preprint arXiv:1706.01905*, 2017.
- [25] A. Pourchot and O. Sigaud. Cem-rl: Combining evolutionary and gradient-based methods for policy search. *arXiv preprint arXiv:1810.01222*, 2018.
- [26] E. Coumans and Y. Bai. Pybullet, a python module for physics simulation for games, robotics and machine learning. <http://pybullet.org>, 2016–2019.
- [27] J. Schulman, S. Levine, P. Abbeel, M. Jordan, and P. Moritz. Trust region policy optimization. In *International conference on machine learning*, pages 1889–1897, 2015.
- [28] T. P. Lillicrap, J. J. Hunt, A. Pritzel, N. Heess, T. Erez, Y. Tassa, D. Silver, and D. Wierstra. Continuous control with deep reinforcement learning. *arXiv preprint arXiv:1509.02971*, 2015.
- [29] V. Mnih, A. P. Badia, M. Mirza, A. Graves, T. Lillicrap, T. Harley, D. Silver, and K. Kavukcuoglu. Asynchronous methods for deep reinforcement learning. In *International conference on machine learning*, pages 1928–1937, 2016.
- [30] J. Schulman, F. Wolski, P. Dhariwal, A. Radford, and O. Klimov. Proximal policy optimization algorithms. *arXiv preprint arXiv:1707.06347*, 2017.
- [31] T. Haarnoja, H. Tang, P. Abbeel, and S. Levine. Reinforcement learning with deep energy-based policies. In *Proceedings of the 34th International Conference on Machine Learning-Volume 70*, pages 1352–1361. JMLR. org, 2017.
- [32] S. Khadka and K. Tumer. Evolution-guided policy gradient in reinforcement learning. In *Advances in Neural Information Processing Systems*, pages 1188–1200, 2018.
- [33] R. J. Williams. Simple statistical gradient-following algorithms for connectionist reinforcement learning. *Machine learning*, 8(3-4):229–256, 1992.
- [34] H. van Hoof, D. Tanneberg, and J. Peters. Generalized exploration in policy search. *Machine Learning*, 106(9-10):1705–1724, oct 2017. Special Issue of the ECML PKDD 2017 Journal Track.
- [35] D. P. Kingma and M. Welling. Auto-encoding variational bayes. *arXiv preprint arXiv:1312.6114*, 2013.
- [36] A. Raffin, A. Hill, M. Ernestus, A. Gleave, A. Kanervisto, and N. Dormann. Stable baselines3. <https://github.com/DLR-RM/stable-baselines3>, 2019.
- [37] A. Hill, A. Raffin, M. Ernestus, A. Gleave, A. Kanervisto, R. Traore, P. Dhariwal, C. Hesse, O. Klimov, A. Nichol, M. Plappert, A. Radford, J. Schulman, S. Sidor, and Y. Wu. Stable baselines. <https://github.com/hill-a/stable-baselines>, 2018.
- [38] A. Raffin. RL baselines zoo. <https://github.com/araffin/rl-baselines-zoo>, 2018.
- [39] J. Reinecke, B. Deutschmann, and D. Fehrenbach. A structurally flexible humanoid spine based on a tendon-driven elastic continuum. In *2016 IEEE International Conference on Robotics and Automation (ICRA)*, pages 4714–4721. IEEE, 2016.

- [40] B. Deutschmann, A. Dietrich, and C. Ott. Position control of an underactuated continuum mechanism using a reduced nonlinear model. In *2017 IEEE 56th Annual Conference on Decision and Control (CDC)*, pages 5223–5230. IEEE, 2017.
- [41] B. Deutschmann, M. Chalon, J. Reinecke, M. Maier, and C. Ott. Six-dof pose estimation for a tendon-driven continuum mechanism without a deformation model. *IEEE Robotics and Automation Letters*, 4(4):3425–3432, 2019.
- [42] M. Bellemare, S. Srinivasan, G. Ostrovski, T. Schaul, D. Saxton, and R. Munos. Unifying count-based exploration and intrinsic motivation. In *Advances in neural information processing systems*, pages 1471–1479, 2016.
- [43] I. Osband, C. Blundell, A. Pritzel, and B. Van Roy. Deep exploration via bootstrapped dqn. In *Advances in neural information processing systems*, pages 4026–4034, 2016.
- [44] M. Fortunato, M. G. Azar, B. Piot, J. Menick, M. Hessel, I. Osband, A. Graves, V. Mnih, R. Munos, D. Hassabis, O. Pietquin, C. Blundell, and S. Legg. Noisy networks for exploration. In *International Conference on Learning Representations*, 2018. URL <https://openreview.net/forum?id=ryWHGPkAW>.
- [45] I. Osband, J. Aslanides, and A. Cassirer. Randomized prior functions for deep reinforcement learning. In *Advances in Neural Information Processing Systems*, pages 8617–8629, 2018.
- [46] F. Sehnke, C. Osendorfer, T. Rückstieß, A. Graves, J. Peters, and J. Schmidhuber. Parameter-exploring policy gradients. *Neural Networks*, 23(4):551–559, 2010.
- [47] H. Mania, A. Guy, and B. Recht. Simple random search provides a competitive approach to reinforcement learning. *arXiv preprint arXiv:1803.07055*, 2018.
- [48] O. Sigaud and F. Stulp. Policy search in continuous action domains: an overview. *Neural Networks*, 2019.
- [49] J. Peters and S. Schaal. Reinforcement learning of motor skills with policy gradients. *Neural networks*, 21(4):682–697, 2008.
- [50] T. Salimans, J. Ho, X. Chen, S. Sidor, and I. Sutskever. Evolution strategies as a scalable alternative to reinforcement learning. *arXiv preprint arXiv:1703.03864*, 2017.
- [51] F. Such, V. Madhavan, E. Conti, J. Lehman, K. Stanley, and J. Clune. Deep neuroevolution: Genetic algorithms are a competitive alternative for training deep neural networks for reinforcement learning. *arXiv preprint arXiv:1712.06567*, 12 2017.
- [52] J. Schulman, P. Moritz, S. Levine, M. Jordan, and P. Abbeel. High-dimensional continuous control using generalized advantage estimation. *arXiv preprint arXiv:1506.02438*, 2015.
- [53] D. Silver, G. Lever, N. Heess, T. Degris, D. Wierstra, and M. Riedmiller. Deterministic policy gradient algorithms. In *Proceedings of the 31st International Conference on International Conference on Machine Learning - Volume 32, ICML14*, page I387I395. JMLR.org, 2014.
- [54] V. Mnih, K. Kavukcuoglu, D. Silver, A. Graves, I. Antonoglou, D. Wierstra, and M. Riedmiller. Playing atari with deep reinforcement learning. *arXiv preprint arXiv:1312.5602*, 2013.
- [55] L. Engstrom, A. Ilyas, S. Santurkar, D. Tsipras, F. Janoos, L. Rudolph, and A. Madry. Implementation matters in deep {rl}: A case study on {ppo} and {trpo}. In *International Conference on Learning Representations*, 2020. URL <https://openreview.net/forum?id=r1etN1rtPB>.
- [56] T. Akiba, S. Sano, T. Yanase, T. Ohta, and M. Koyama. Optuna: A next-generation hyperparameter optimization framework. In *Proceedings of the 25rd ACM SIGKDD International Conference on Knowledge Discovery and Data Mining*, 2019.
- [57] F. Pardo, A. Tavakoli, V. Levдик, and P. Kormushev. Time limits in reinforcement learning. *arXiv preprint arXiv:1712.00378*, 2017.

- [58] A. Rajeswaran, K. Lowrey, E. V. Todorov, and S. M. Kakade. Towards generalization and simplicity in continuous control. In *Advances in Neural Information Processing Systems*, pages 6550–6561, 2017.
- [59] D. P. Kingma and J. Ba. Adam: A method for stochastic optimization. *arXiv preprint arXiv:1412.6980*, 2014.

A Supplementary Material

A.1 Algorithms

In this section, we shortly present the algorithms used in this paper. They correspond to state of the art methods in model-free RL for continuous control, either in terms of sample efficiency or wall-clock time.

A2C A2C is the synchronous version of Asynchronous Advantage Actor-Critic (A3C) [29]. It is an actor-critic method that uses parallel rollouts of n -steps to update the policy. It relies on the REINFORCE [33] estimator to compute the gradient. A2C is fast but not sample efficient.

PPO A2C gradient update does not prevent large changes that lead to huge drop in performance. To tackle this issue, Trust Region Policy Optimization (TRPO) [27] introduces a trust-region in the policy parameter space, formulated as a constrained optimization problem: it updates the policy while being close in terms of KL divergence to the old policy. Its successor, Proximal Policy Optimization (PPO) [30] relaxes the constrain (which requires costly conjugate gradient step) by clipping the objective using importance ratio. PPO makes also use of workers (as in A2C) and Generalized Advantage Estimation (GAE) [52] for computing the advantage.

TD3 Deep Deterministic Policy Gradient (DDPG) [28] combines the deterministic policy gradient algorithm [53] with the improvements from Deep Q-Network (DQN) [54]: using a replay buffer and target networks to stabilize training. Its direct successor, Twin Delayed DDPG (TD3) [6] brings three major tricks to tackle issues coming from function approximation: clipped double Q-Learning (to reduce overestimation of the Q-value function), delayed policy update (so the value function converges first) and target policy smoothing (to prevent overfitting). Because the policy is deterministic, DDPG and TD3 rely on external noise for exploration.

SAC Soft Actor-Critic [31], successor of Soft Q-Learning (SQL) [17] optimizes the maximum-entropy objective, that is slightly different compared to the classic RL objective:

$$J(\pi) = \sum_{t=0}^T \mathbb{E}_{(\mathbf{s}_t, \mathbf{a}_t) \sim \rho_\pi} [r(\mathbf{s}_t, \mathbf{a}_t) + \alpha \mathcal{H}(\pi(\cdot | \mathbf{s}_t))]. \quad (11)$$

where \mathcal{H} is the policy entropy and α is the entropy temperature and allows to have a trade-off between the two objectives.

SAC learns a stochastic policy, using a squashed Gaussian distribution, and incorporates the clipped double Q-learning trick from TD3. In its latest iteration [8], SAC automatically adjusts the entropy coefficient α , removing the need to tune this crucial hyperparameter.

Which algorithm for robotics? A2C and PPO are both on-policy algorithms and can be easily parallelized, resulting in relatively small training time. On the other hand, SAC and TD3 are off-policy and run on a single worker, but are much more sample efficient than the two previous methods, achieving equivalent performances with a fraction of the samples.

Because we are focusing on robotics applications, having multiple robots is usually not possible, which makes TD3 and SAC the methods of choice. Although TD3 and SAC are very similar, SAC embeds the exploration directly in its objective function, making it easier to tune. We also found, during our experiments in simulation, that SAC works for a wide range of hyperparameters. As a result, we adopt that algorithm for the experiment on a real robot and for the ablation study.

A.2 Implementation Details

We used a PyTorch [36] version of Stable-Baselines [37] library, with results matching the ones published in the RL zoo [38]. The training scripts are available at <https://github.com/DLR-RM/rl-baselines3-zoo/tree/sde> and implementation at <https://github.com/DLR-RM/stable-baselines3/tree/sde>. It uses the common implementations tricks for PPO [55] for the version using independent Gaussian noise.

For SAC, to ensure numerical stability, we clip the mean to be in range $[-2, 2]$, as it was causing infinite values. In the original implementation, a regularization \mathcal{L}_2 loss on the mean and standard deviation was used instead. The algorithm for SAC with gSDE is described in Algorithm 1.

Compared to the original SDE paper, we did not have to use the *expln* trick [1] to avoid exploding variance for PyBullet tasks. However, we found it useful on specific environment like *BipedalWalkerHardcore-v2*. The original SAC implementation clips this variance.

Algorithm 1 Soft Actor-Critic with gSDE

```
Initialize parameters  $\theta_\mu, \theta_Q, \sigma, \alpha$ 
Initialize replay buffer  $\mathcal{D}$ 
for each iteration do
     $\theta_\epsilon \sim \mathcal{N}(0, \sigma^2)$  ▷ Sample noise function parameters
    for each environment step do
         $\mathbf{a}_t = \pi(\mathbf{s}_t) = \mu(\mathbf{s}_t; \theta_\mu) + \epsilon(\mathbf{s}_t; \theta_\epsilon)$  ▷ Get the noisy action
         $\mathbf{s}_{t+1} \sim p(\mathbf{s}_{t+1} | \mathbf{s}_t, \mathbf{a}_t)$  ▷ Step in the environment
         $\mathcal{D} \leftarrow \mathcal{D} \cup \{(\mathbf{s}_t, \mathbf{a}_t, r(\mathbf{s}_t, \mathbf{a}_t), \mathbf{s}_{t+1})\}$  ▷ Update the replay buffer
    end for
    for each gradient step do
         $\theta_\epsilon \sim \mathcal{N}(0, \sigma^2)$  ▷ Sample noise function parameters
        Sample a minibatch from the replay buffer  $\mathcal{D}$ 
        Update the entropy temperature  $\alpha$ 
        Update parameters using  $\nabla J_Q$  and  $\nabla J_\pi$  ▷ Update actor  $\mu$ , critic  $Q$  and noise variance  $\sigma$ 
        Update target networks
    end for
end for
```

A.3 Learning Curves

Figure 5 and Figure 6 show the learning curves for off-policy and on-policy algorithms on the four PyBullet tasks, using gSDE or unstructured Gaussian exploration.

A.4 Ablation Study: Additional Plots

Figure 7 displays the ablation study on remaining PyBullet tasks. It shows that SAC is robust against initial exploration variance, and PPO results highly depend on the sampling frequency.

Figure 8 shows the effect of parallel sampling for A2C. The benefit is only clearly visible for the HALFCHEETAH task. On the other, this parameter does not really affects the final performance.

A.5 Hyperparameter Optimization

To tune the hyperparameters, we use a TPE sampler and a median pruner from Optuna [56] library. We give a budget of 500 candidates with a maximum of $3 \cdot 10^5$ time-steps on the HALFCHEETAH environment. Some hyperparameters are then manually adjusted (e. g. increasing the replay buffer size) to improve the stability of the algorithms.

A.6 Hyperparameters

For all experiments with a time limit, as done in [3, 57, 58, 37], we augment the observation with a time feature (remaining time before the end of an episode) to avoid breaking Markov assumption. This feature has a great impact on performance, as shown in Figure 9b.

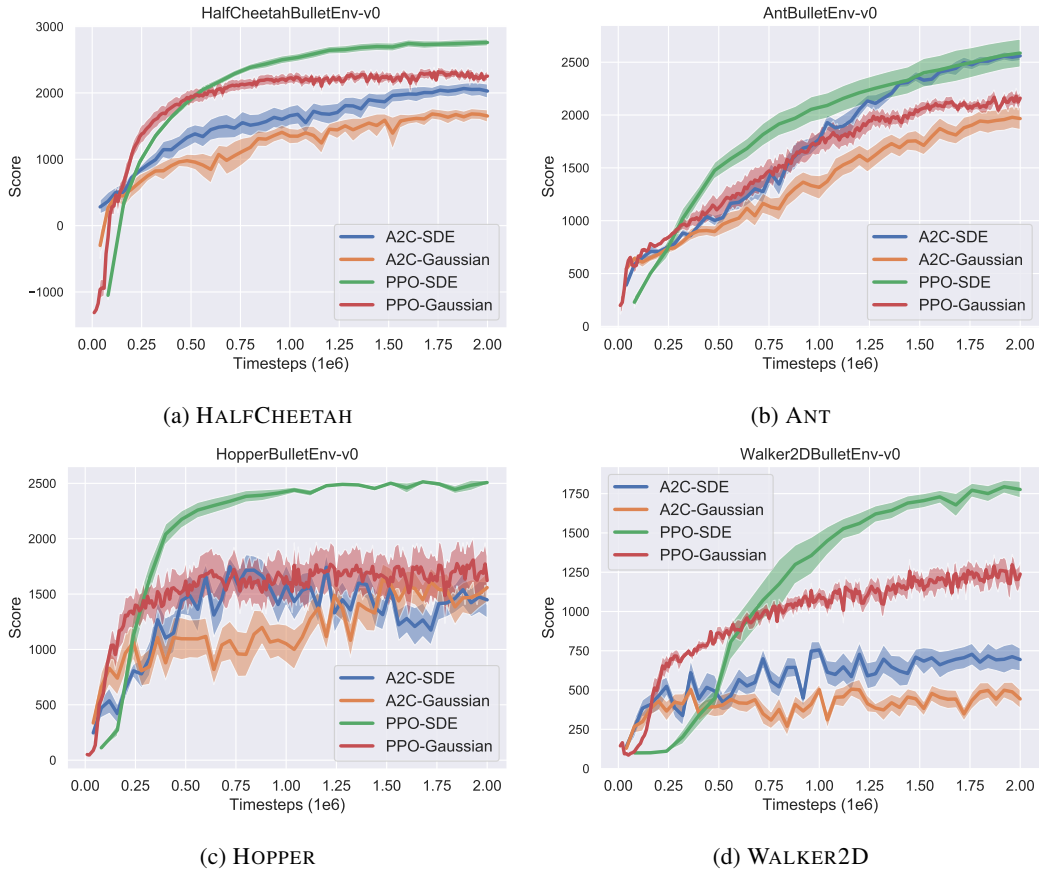


Figure 5: Learning curves for on-policy algorithms on PyBullet tasks. The line denotes the mean over 10 runs of 2 million steps.

Figure 9a displays the influence of the network architecture for SAC on PyBullet tasks. A bigger network usually yields better results but the gain is minimal passed a certain complexity (here, a two layers neural network with 256 unit per layer).

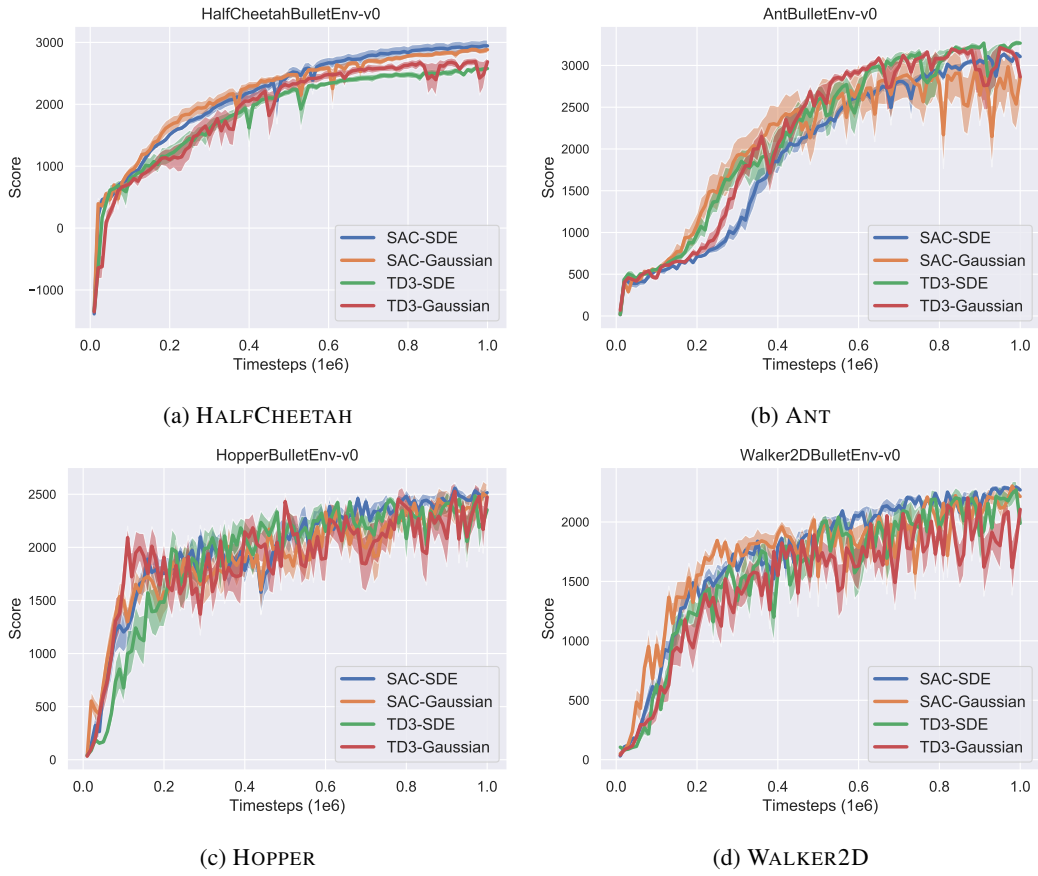


Figure 6: Learning curves for off-policy algorithms on PyBullet tasks. The line denotes the mean over 10 runs of 1 million steps.

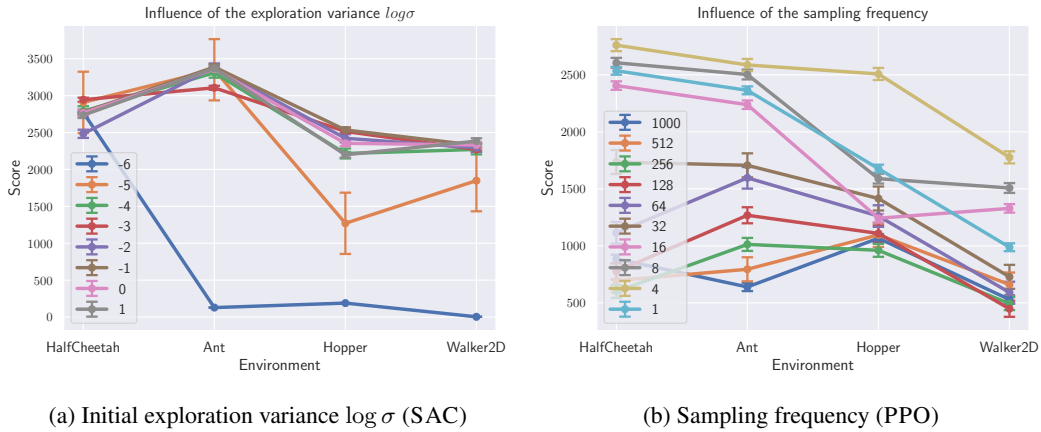


Figure 7: Sensitivity of SAC and PPO to selected hyperparameters on PyBullet tasks

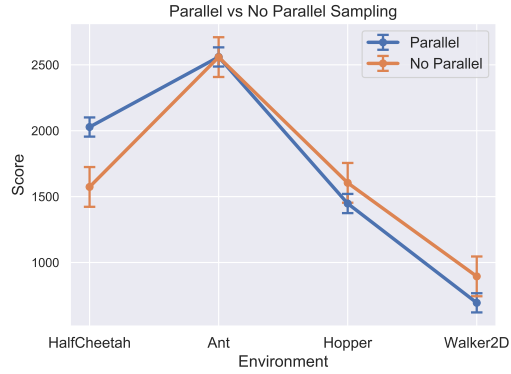
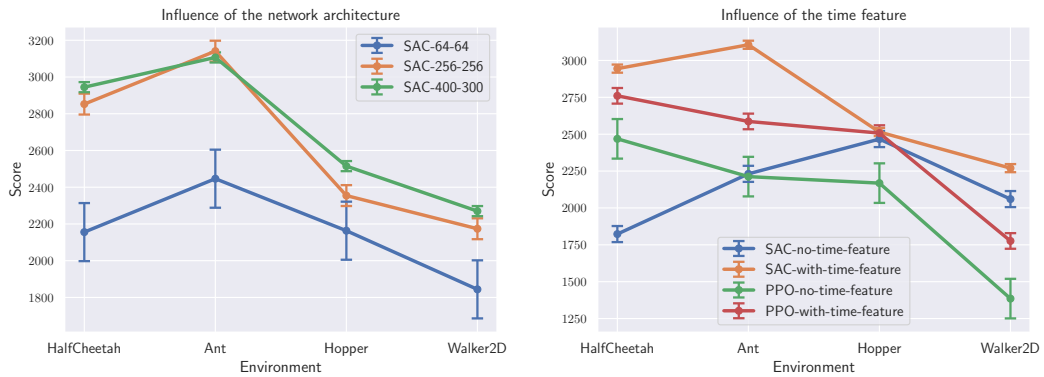


Figure 8: Effect of parallel sampling for A2C on PyBullet tasks



(a) Influence of the network architecture

(b) Influence of the time feature

Figure 9: (a) Influence of the network architecture (same for actor and critic) for SAC on PyBullet environments. The labels displays the number of units per layer. (b) Influence of including the time or not in the observation for PPO and SAC.

Table 3: SAC Hyperparameters

Parameter	Value
<i>Shared</i>	
optimizer	Adam [59]
learning rate	$7.3 \cdot 10^{-4}$
learning rate schedule	constant
discount (γ)	0.98
replay buffer size	$3 \cdot 10^5$
number of hidden layers (all networks)	2
number of hidden units per layer	[400, 300]
number of samples per minibatch	256
non-linearity	<i>ReLU</i>
entropy coefficient (α)	auto
target entropy	$-\dim(\mathcal{A})$
target smoothing coefficient (τ)	0.02
target update interval	64
train frequency	64
gradient steps	64
warm-up steps	10 000
normalization	None
<i>gSDE</i>	
initial $\log \sigma$	-3

Table 4: SAC Environment Specific Parameters

Environment	Learning rate schedule
HopperBulletEnv-v0	linear
Walker2dBulletEnv-v0	linear

Table 5: TD3 Hyperparameters

Parameter	Value
<i>Shared</i>	
optimizer	Adam [59]
discount (γ)	0.98
replay buffer size	$2 \cdot 10^5$
number of hidden layers (all networks)	2
number of hidden units per layer	[400, 300]
number of samples per minibatch	100
non-linearity	<i>ReLU</i>
target smoothing coefficient (τ)	0.005
target policy noise	0.2
target noise clip	0.5
policy delay	2
warm-up steps	10 000
normalization	None
<i>gSDE</i>	
initial $\log \sigma$	-3.62
learning rate for TD3	$6 \cdot 10^{-4}$
target update interval	64
train frequency	64
gradient steps	64
learning rate for gSDE	$1.5 \cdot 10^{-3}$
<i>Unstructured Exploration</i>	
learning rate	$1 \cdot 10^{-3}$
action noise type	Gaussian
action noise std	0.1
target update interval	every episode
train frequency	every episode
gradient steps	every episode

Table 6: A2C Hyperparameters

Parameter	Value
<i>Shared</i>	
number of workers	4
optimizer	RMSprop with $\epsilon = 1 \cdot 10^{-5}$
discount (γ)	0.99
number of hidden layers (all networks)	2
number of hidden units per layer	[64, 64]
shared network between actor and critic	False
non-linearity	<i>Tanh</i>
value function coefficient	0.4
entropy coefficient	0.0
max gradient norm	0.5
learning rate schedule	linear
normalization	observation and reward [37]
<i>gSDE</i>	
number of steps per rollout	8
initial log σ	-3.62
learning rate	$9 \cdot 10^{-4}$
<i>GAE</i> coefficient [52] (λ)	0.9
orthogonal initialization [55]	no
<i>Unstructured Exploration</i>	
number of steps per rollout	32
initial log σ	0.0
learning rate	$2 \cdot 10^{-3}$
<i>GAE</i> coefficient [52] (λ)	1.0
orthogonal initialization [55]	yes

Table 7: PPO Hyperparameters

Parameter	Value
<i>Shared</i>	
optimizer	Adam [59]
discount (γ)	0.99
value function coefficient	0.5
entropy coefficient	0.0
number of hidden layers (all networks)	2
shared network between actor and critic	False
max gradient norm	0.5
learning rate schedule	constant
advantage normalization [37]	True
clip range value function [55]	no
normalization	observation and reward [37]
<i>gSDE</i>	
number of workers	16
number of steps per rollout	512
initial log σ	-2
gSDE sample frequency	4
learning rate	$3 \cdot 10^{-5}$
number of epochs	20
number of samples per minibatch	128
number of hidden units per layer	[256, 256]
non-linearity	<i>ReLU</i>
GAE coefficient [52] (λ)	0.9
clip range	0.4
orthogonal initialization [55]	no
<i>Unstructured Exploration</i>	
number of workers	1
number of steps per rollout	2048
initial log σ	0.0
learning rate	$2 \cdot 10^{-4}$
number of epochs	10
number of samples per minibatch	64
number of hidden units per layer	[64, 64]
non-linearity	<i>Tanh</i>
GAE coefficient [52] (λ)	0.95
clip range	0.2
orthogonal initialization [55]	yes

Table 8: PPO Environment Specific Parameters

Environment	Learning rate schedule	Clip range schedule	initial log σ
<i>gSDE</i>			
AntBulletEnv-v0	default	default	-1
HopperBulletEnv-v0	default	linear	-1
Walker2dBulletEnv-v0	default	linear	default
<i>Unstructured Exploration</i>			
Walker2dBulletEnv-v0	linear	default	default